Available online at **www.ijmrhs.com**

ISSN No: 2319-5886

International Journal of Medical Research & Health Sciences, 2021, 10(10): 1-17

Exploring the Therapeutic and Biomedical Potential of Silver Nanoparticles Biosynthesized by Phycocyanin Extracts from a Marine Cyanobacteria

Rupali Kaur[1], Shailendra Kumar Singh[1], Abhishek Bharadwaj[2], Iffat Zareen Ahmed[3] and Shanthy Sundaram[1*]

[1]Centre of Biotechnology, University of Allahabad, Prayagraj, Uttar Pradesh, India

[2]Department of Environmental Science, Amity University, Gwalior, Madhya Pradesh, India

[3]Department of Bioengineering, Integral University, Dasauli, Kursi Road, Lucknow, Uttar Pradesh, India

[*]Corresponding e-mail: shanthy.cbt@gmail.com

ABSTRACT

The study aimed to synthesize phycocyanin-mediated silver nanoparticles (Ag-CNPs) using pigment extracts from Synechococcus BDUSM13 as a green nano-synthesis procedure, an alternative for the toxic chemical route. Biosynthesized Ag-CNPs were characterized and analyzed for their therapeutic (e.g. antibacterial) and biomedical (e.g. anticancer) potential. Ag-CNPs were spherical in shape, crystalline, and small width-to-length ratio with a 4 nm to 20.9 nm diameter range. They also unveiled a wide range of inhibition spectrum activity against clinical bacterial strains such as Campylobacter sp., Shigella sp., Salmonella typhi, Bacillus subtilis, and Klebsiella sp. Ag-CNPs showed the highest inhibition against Klebsiella (13.5 mm) and B. subtilis (13.3 mm) strains whereas the lowest zone of inhibition was observed against Shigella (8.0 mm) at 100 µg/mL Ag-CNPs. The cytotoxic analysis on the MDA-MBA-231 cancer cell line revealed that the proliferation rate was declined gradually with higher Ag-CNPs concentrations. The viability of cancer cells was also reduced from 80.15% to 29.12%, 41.42% to 18.12%, and 25.12% to 5.5%, respectively, after 24, 48, and 72 hrs of incubation. Quantitative verification of reactive oxygen species showed a 195.4% increase in ROS production with 38.9 µg/mL of Ag-CNPs in comparison to control cells. The study indicates that due to the strong antibacterial and anti-cancerous activity of Ag-CNPs, it could be employed as a novel antimicrobial and anticancer agents.

Keywords: Cyanobacteria, Antimicrobial, Anticancer, Silver nanoparticles

INTRODUCTION

Extraordinary characteristics of Metal Nanoparticles (MNPs) have recently become the focus of researchers from all over the world to explore its immense applications. Structurally, MNPs are composed of an inorganic metal or metal oxide core covered with a shell made up of organic or inorganic material or metal oxide. These exhibit improved properties to their respective metal source based on their size, distribution, architecture, chemical assembly, colloidal stability, and biocompatibility. Currently, MNPs are widely synthesized by conventional physical and chemical routes; pose various biological risks and adverse effects to living cells. Consequently, there is an intensive need for environmentally friendly, safe, consistent, and clean routes for MNPs synthesis. In this regard, biological routes (e.g. extracellular and intracellular) are considered nontoxic thus gaining momentum as an alternative approach for nanoparticle preparations. Biologically MNPs are not only synthesized rapidly in a cost-effective manner but also discharge safely in the surroundings without any ecological risks. Extracts of plants, enzymes, and microorganisms such as bacteria, algae, fungi have been successfully utilized as reducing and capping agents for the biosynthesis MNPs [1-5]. Though globally great advances have been made in the screening of various biological systems for the manufacturing of MNPs, there is still a great lack of knowledge about the algae-based biological synthesis of noble

metal nanoparticles. Amongst algal systems used, cyanobacteria "blue-green algae" have been reported as the best biological system for the biosynthesis of MNPs by both pathways, intracellularly and extracellularly. Cyanobacterial extracts as C-Phycocyanin (C-PC) and polysaccharides can extracellularly reduce metal ions. In addition, they can also bio-remediate toxic metals, subsequently converting them to more acceptable forms for human health and the environment. Scientific reports have been published regarding cyanobacteria-based MNPs synthesis, characterization, and applications [6-12].

Although scientific reports are available on cyanobacteria-based MNPs synthesis and characterization, an extensive understanding of the MNPs applications is required before large-scale commercial production. Cyanobacteria have been shown the ability to produce MNPs with a wide range of metals such as gold, silver, cadmium, and platinum [6,13-15]. Amongst metals used, silver (AgNPs) is the most abundantly used MNPs. They are known for their antimicrobial properties and have geared research interests towards antibacterial and antifungal agents. Silver, one of the most abundantly used noble metals, has high conductivity and promising photocatalytic activity. Their large surface area to volume ratio allows AgNPs to encounter the microbial or living cells with a higher percentage of interaction than larger particles of the same parent material. Though unique properties of AgNPs have been geared towards research interests towards biomedical and therapeutic applications, the low colloidal stability of these materials sends them to aggregate at biological pH. Cyanobacteria-based MNPs may solve this problem with their phytochemical moieties like phycocyanin and polysaccharides, increasing the biocompatibility of these materials by surface modifications.

This study has investigated the biosynthesis of AgNPs through phycocyanin extracted from marine cyanobacteria *Synechococcus* BDUSM13. Synthesized MNPs were characterized and analyzed for their potential for biomedical (e.g. anticancer) and therapeutic (e.g. antibacterial) applications.

MATERIALS AND METHODS

Chemicals and Reagents

Analytical grade chemicals were used for reagents preparation in double-distilled water (Milli-Q grade water, Merck). Silver nitrate ($AgNO_3$, 99.98 %) for nanoparticle biosynthesis was purchased from Sigma Aldrich, St. Louis. Growth media for the microorganisms such as Nutrient Agar (NA), Mueller Hinton Broth (MHB), and Mueller Hinton Agar (MHA) were procured from Hi-Media Pvt. Ltd., India. Before the experiments, glassware was washed with chromic acid (Hi-Media, Mumbai, India), sterilized using an autoclave, and dried in a hot air oven. All the experiments were performed in triplicates and the results were expressed as mean ± SD (Standard Deviation) of all concentrations. The selected cell line, MDA-MB-231 was cultured in Dulbecco's Modified Eagles Medium (DMEM) media (Sigma-Aldrich) supplemented with Fetal Bovine Serum (FBS) (Invitrogen), 2 mM L-glutamine (Sigma-Aldrich), sodium bicarbonate (Sigma Aldrich), and 10 U/mL penicillin and streptomycin (Sigma-Aldrich) and maintained in a humidified 5% CO_2 incubator, 3-(4,5-dimethylthiazol-2-yl)-2,5-diphenyltetrazolium bromide (MTT) were purchased from Sigma-Aldrich.

Sources, Growth and Culture Conditions of Microorganisms

A marine cyanobacterium, *Synechococcus* BDUSM-13, was obtained from National Facility for Marine Cyanobacteria (NFMC) Tiruchirappalli, India, and maintained in ASN^{+ve} at Advanced Laboratory for Phycological Assessment (ALPHA plus), Centre of Biotechnology, University of Allahabad, India. Cultures were grown for 14 days in autoclaved 250 mL conical flasks containing 150 mL of medium, pH 7.5, under 20 ± 2℃ temperatures, and light intensity of 72 $\mu E/m^2/s$ with a dark: the light cycle of 16:8 hrs. During the log phase of growth, cyanobacterial cells were harvested by centrifugation at 4000 g in a refrigerated centrifuge (Remi, India) at 4°C for 20 min. Harvested biomass was dried at 40℃ for 48 hrs, and stored at 4℃ till pigment extraction. Five different pathogenic bacterial strains from two large bacterial taxonomic lineages, gram-positive (*Bacillus subtilis*) and gram-negative (*Salmonella typhi*, *Klebsiella pneumoniae*, *Campylobacter* sp., and *Shigella* sp.) were selected for antibacterial experiments. The lyophilized strains were procured from the National Collection of Industrial Microorganisms (NCIM), Pune, India, and revived on nutrient agar as prescribed at Advanced Laboratory for Phycological Assessment (ALPHA plus), University of Allahabad, India.

Extraction, Purification, and Quantification of C-phycocyanin

C-PC was extracted by methods given by Soni [16]. Harvested cell pellets were washed in 30 mL 0.1 M Na-phosphate buffer (pH 7) and crushed in mortar and pestle by addition of liquid nitrogen. Finely powdered frozen cell mass was further thawed by the addition of 100 mL of the phosphate buffer, containing 10 mm EDTA. To remove the cell debris from the buffer, the slurry was centrifuged at 10,000 g for 20 min. Blue supernatant-crude cell-free extract was removed carefully by using a micropipette and used further for purification steps. Purification of crude C-PC was carried out at 4℃ by ammonium sulfate precipitation in an icebox followed by gel filtration chromatography (Biorad, India) [17]. High purity C-PC fractions were pooled together, lyophilized, and stored in dark at 4℃ in a refrigerator (Godrej, India) for further study. The protein estimation of purified C-PC fractions was carried out by the Lowry method [18]. UV-VIS absorbance spectra were also recorded on a double-beam1800 UV-vis spectrophotometer (Shimadzu, Kyoto, Japan). The spectra were recorded in the wavelength range of (200-800) nm at fast scan speed mode at default settings of the spectrophotometer. The C-phycocyanin concentration (C-PC) in mg/mL was calculated from the optical densities at 652 nm and 620 nm, using Equation 1 [19]. The extraction yield was calculated using Equation 2 [20].

$$CPC = \frac{(OD_{620} - 0.474OD_{652})}{5.34} \qquad (Equation\ 1)$$

$$Yield = \frac{(CPC)V}{DB} \qquad (Equation\ 2)$$

Where, yield=the extraction yield of phycocyanin in mg of C-phycocyanin/dry biomass (g), V=the solvent volume (mL), and DB=Dry Biomass (g).

Green Biosynthesis of MNPs from C-phycocyanin

Synthesis of phycocyanin silver nanoparticles was done employing 10 mL of pure phycocyanin and 1 mL aqueous $AgNO_3$ solution (5 mM), pH 7. The purity of pigment was checked by finding the ratio of absorbance at 620 and 280, respectively. This reaction mixture was left for incubation at 25℃ in white cool fluorescent light at 40 mmol photons/m^2/s or kept in dark for 48 hours. The formation of silver nanoparticles was noticed by a change in colour to brownish for silver nanoparticles. After that culture solution was centrifuged for 7500 rpm for 15 min in a refrigerated centrifuge (Remi, India). For control, fresh media with the addition of $AgNO_3$ was employed. In addition, a commercially available C-phycocyanin from *Spirulina* sp. was purchased from Sigma Aldrich.

Characterization of Biosynthesized Ag-CNPs

The biosynthesis of Ag-CNPs in the reaction mixture was monitored for the stability of nanoparticle solutions by measuring the UV-Vis spectrum. An aliquot of 0.1 mL was drawn at regular intervals and a UV-Vis absorbance spectrum was recorded on UV-Vis spectrophotometer from λ_{200} to λ_{800} nm wavelength range. All measurements were recorded in triplicate at room temperature using a 1 cm path length quartz cuvette. $AgNO_3$ solutions were used as a control throughout the experiment. Before particle size and zeta potential measurements, Ag-CNPs were suspended in double distilled water at a concentration of 100 mg/L and then sonicated using a sonicator (Sonics, Model VCX 130) at room temperature for 20 min at 40 W to form a homogeneous suspension. Both particle size and zeta potential measurements were determined using Zetasizer Nano ZS 90 (Malvern Instruments, Worcestershire, UK). For these experiments, Asymmetrical Flow Field-Flow Fractionation (AF_4) was directly interfaced to a zeta sizer without channel split and the detector flow was set to 1.0 mL/min for all fractions. For particle size measurement, Ag-CNPs in liquid suspension was separated by the AF_4 system at 25℃ and then measured by Dynamic Light Scattering (DLS) method. In DLS, a 632 nm, He-Ne laser was used as the light source which is scattered through Ag-CNPs of liquid suspension. The scattered light was collected at a 173º scattering angle and backscatter detection was performed by an Avalanche Photodiode (APD). All experiments were carried out in triplicate and the average hydrodynamic diameter results presented are the average measurements of the 10 runs with standard deviation in flow mode of DLS detector using a quartz flow-through cell (Hellma, Germany) [21]. Electrophoretic Light Scattering (ELS) method was utilized for measurement of surface zeta potential (ζP) of Ag-CNPs (particle concentration c_p=25 mg/L^1, T=24.8℃ and pH 9.2) with sample size no larger than 4 mm × 7mm × 1.5 mm (L × W × H). Surface zeta potential was measured

by the methodology developed by Malvern Instruments [22]. A surface zeta potential dip cell (ZEN1002, Malvern Instruments, UK) attached with a pair of palladium electrodes was used to provide an electrical trigger on charged Ag-CNPs. The signals were collected at a 12.8º angle and the data were analyzed using Zetasizer Software. The zeta potential transfer standard (DTS1235, Malvern Instruments) was used as a tracer particle (zeta potential= -42.0 mV ± 4.2 mV, pH 9.2).

The elemental composition of Ag-CNPs with reduced ions was identified by Energy Dispersive X-Ray Analysis (EDXA spectrometer, USA), at Electron Microscope Unit, Banaras Hindu University, Varanasi, India. Before EDX analysis, lyophilized Ag-CNPs powder was compressed using Atlas Manual Hydraulic Press (PRESS-200) to form a 1 mm thick disc in the carbon-coated copper grid (Bruker AXS Inc. USA, Quantax-200) which assure the presence of constituent elements. The acquisition time ranged from 60 s to 100 s with an accelerating voltage of 20 kV. The crystallographic structure of Ag-CNPs was determined by X-ray Diffraction Analysis (XRD) technique by Rigaku Multi-Flex X-ray diffractometer (Rigaku, Tokyo, Japan) at MNIT Allahabad. The device was operated with a sealed X-ray tube at 40 kV, 40 mA, for 6°/min scanning rate, and 2θ diffraction angles ranged from 20° to 80° with CuKα (k=1.54 Å), the wavelength of the x-ray source. Subsequently, more information on morphology, composition, and crystalline nature of biosynthesized Ag-CNPs was obtained by Transmission Electron Microscopy (TEM) (JEOL-JEM-100 CXII instrument) analysis at Banaras Hindu University, Varanasi, India. TEM is a direct and effective approach to determine the particle size and morphology of the nanoparticles. The crystalline nature was examined with the help of the Selected Area Electron Diffraction (SAED) pattern by TEM. The average size of MNPs was calculated by counting at least 100 NPs. Moreover, functional groups which are responsible for the reduction of metals (silver) to form stable MNPs, detected by Fourier-Transform Infrared (FTIR) spectrophotometer (FTIR 4600, JASCO, Japan) (University of Allahabad). Freeze-dried Ag-CNPs were mixed with potassium bromide (ratio 1:100) to make a pellet and then spectrum was recorded in the range from 599/cm to 4000/cm at 4/cm resolutions.

Antibacterial Potential of Biosynthesized Ag-CNPs

Antibacterial activity of Ag-CNPs was tested by the disk-diffusion system (Kirby-Bauer method), described by Nathan, against four gram-negative and one gram-positive pathogenic bacterial strains; namely, *Shigella sp*., *S. typhi*, *K. pneumoniae*, *Campylobacter sp*. and *B. subtilis*, respectively [23]. Before the assay, each test organism was grown in Nutrient Broth (DifcoTM) at 28 ± 1ºC for 24 hrs. Agar wells (8 mm in diameter) were prepared ingrown bacterial lawns of agar plates with a sterilized cork-borer device. Antibacterial activity of biosynthesized Ag-CNPs was tested in three different concentrations i.e., 25, 50, and 100 µg/mL added in the agar wells. $AgNO_3$ was used as a positive control ((+) C). The agar plates were incubated at 37°C for 24 hrs and then examined for the presence of inhibition zones. The diameters of inhibition zones around the agar wells were measured and the mean value for each bacterium was recorded (in millimeter).

Test for Anticancer Activity of Biosynthesized MNPs

Cancer cells and cell culture reagents: The cancer cell line, MDA-MB-231 (human triple-negative breast cancer cells) was purchased from the Cell Repository Center, National Centre for Cell Sciences (NCCS), Pune, India. The cancer cells were maintained in DMEM/F-12 (1:1) media, supplemented with 2 mM of L-glutamine and Balanced Salt Solution (BSS), 1.5 g/L Na_2CO_3, 0.1 mM non-essential amino acids, 1 mM sodium pyruvate, 2 mM L-glutamine, 1.5 g/L glucose, 10 mM HEPES and 10% heat-inactivated Fetal Bovine Serum (FBS) and 1% antibiotic mixture (penicillin G and streptomycin-100 IU/100 lg) solution. All chemicals in the experiments were analytical grade, supplied by Sigma-Aldrich. The cells were maintained at 37°C with 5% CO_2 in a humidified CO_2 incubator (Thermo Scientific, USA).

Cytotoxicity of Ag-CNPs by MTT assay: The *in vitro* cytotoxicity and survival of cells against biosynthesized Ag-CNPs were measured by MTT (dimethylthiazol-diphenyltetrazolium bromide) assay [24,25]. The MTT is a colorimetric assay that determines the functional state of mitochondria, indicating cell viability. The test was performed in a 96 well plate, contained controls, and different concentration series (1, 3, 5, 10, 25, and 50 µg/mL) of C-PC extract, Ag-CNPs (dissolved in Phosphate Buffer Saline (PBS), with three replicates each. MDA-MB-231 cells were grown (1×10^4 cells/well) in a 96-well plate for 24, 48, and 72 hrs at 37°C with 75% confluence. PBS without C-PC and Ag-CNPs was used as control. The medium was replaced in each experimental set with a fresh DMEM medium (2 mL) after

18 hours of incubation. After the end of experiments, plates were washed with sterile PBS to remove cell debris and excess nanoparticles from each well, before MTT assay. The assay was performed by adding 50 µl of MTT reagent (5µg/mL) and incubated further for 5 hrs at 37°C in the CO_2 incubator. The MTT solution was then discarded, and DMSO (500 µL) was added. The plates were placed on a shaker for at least 10 minutes to solubilize the formations of purple crystal formazan. The absorbance was measured at a wavelength of 570 nm and 630 nm using a multi-well microplate reader (Synergy HT, Bio-Tec, USA). The results were used to construct a graph of cell viability percentage against C-PC extract and Ag-CNPs concentrations using Equation 3 [26].

$$Cytotoxicity\ (\%) = \frac{(OD_{Treated} - OD_{Blank})}{(OD_{Control} - OD_{Blank})} \times 100 \qquad Equation\ 3$$

Intracellular reactive oxygen species estimation: The effect of Ag-CNPs on intracellular Reactive Oxygen Species (ROS) levels of MDA-MB-231 cells were estimated using DCFH-DA dye by fluorescence microscopy imaging and flow cytometry techniques [27]. The cells were inoculated (1×10^5 per well) in 96-well culture plates and allowed to acclimatize for 24 hrs in a CO_2 incubator at 37°C. Afterwards, cells were exposed with Ag-CNPs at IC_{50} and sub-IC_{50} values for 24 and 48 hrs. The intracellular fluorescence intensity of cells was visualized by using an inverted fluorescence microscope (Nikon ECLIPSE Ti-S, Tokyo, Japan). To quantify ROS intensity, both treated and untreated cells were harvested and washed with PBS and incubated in PBS containing 10 µM Dichloro-Dihydro-Fluorescein Diacetate (DCFH-DA) dye at 37°C for 30 min. Subsequently, cells were washed twice with PBS and subjected to flow cytometry analysis. Multi-Mode Microplate Reader (SpectraMax Paradigm, Molecular Devices, USA) was used to estimate the fluorescence intensity with an excitation wavelength of 485 nm and emission wavelength of 535 nm. ROS generation was quantified using Image J software (Image J, National Institutes of Health, and Bethesda, MD). Data were expressed as a percentage of fluorescence intensity relative to the control wells.

Statistical Analysis

All the experiments were done in triplicates, and the results were expressed as mean ± standard error (SD). The statistical software Graph Pad Prism version 5.0 (Graph Pad Software, USA) was used for analysis. p-values were determined using the student t-test; p-value ≤ 0.05 was considered significant.

RESULTS AND DISCUSSION

Spectral Characteristics of C-phycocyanin Extract and Biosynthesized M-CNPs

Cyanobacteria possess water-soluble proteins, Phycobiliproteins (PBPs), a group of light-harvesting accessory pigments which capture light energy to pass on to chlorophylls during photosynthesis. According to their spectral region, they are further classified majorly into three pigments: phycocyanin (PC) λ_{Amax}=610 nm-620 nm, phycoerythrin (PE) λ_{Amax}=(540-570) nm and Allophycocyanin (APC) λ_{Amax}=(650-655) nm. These brilliantly coloured pigments help in the photosynthesis of cyanobacteria to take over a broad range (450 to 650) nm of the solar spectrum. In this study, phycocyanin extracted from Synechococcus BDUSM-13has λ_{Amax}=589 nm as shown in Figure 1. However, during incubation with $AgNO_3$ solutions, C-phycocyanin lost its characteristic absorbance at 589 nm and λ_{Amax} shifted to 440 nm for Ag-CNPs. It indicates pigment was denatured by $AgNO_3$ and MNPs were biosynthesized. Transformation at nanoscale also modifies the optical properties of MNPs, shown by plasmonically generated unique colours. Nanoparticles appear in certain colours because they reflect (scatter) and absorb specific wavelengths of visible light. In this study, rapid reduction of Ag^+ ions into silver nanoparticles was detected by a colour change in the reaction mixture from transparent-blue (C-phycocyanin) to yellowish-brown, due to unaggregated silver nanoparticles (Figure 1). Conversely, no change in colour was observed in aqueous $AgNO_3$ incubated without phycocyanin under the same conditions. Furthermore, nanospheres primarily absorb light and have peaks near 400 nm, indicating the nano size of synthesized Ag-CNPs. Paramelle showed that smaller silver nanospheres primarily absorb light and have peaks near 400 nm, while larger spheres exhibit increased scattering and have peaks that broaden and shift towards longer wavelengths. In our case, λ_{Amax} of Ag-CNPs was 440 nm, showing the synthesis of smaller silver nanospheres [28].

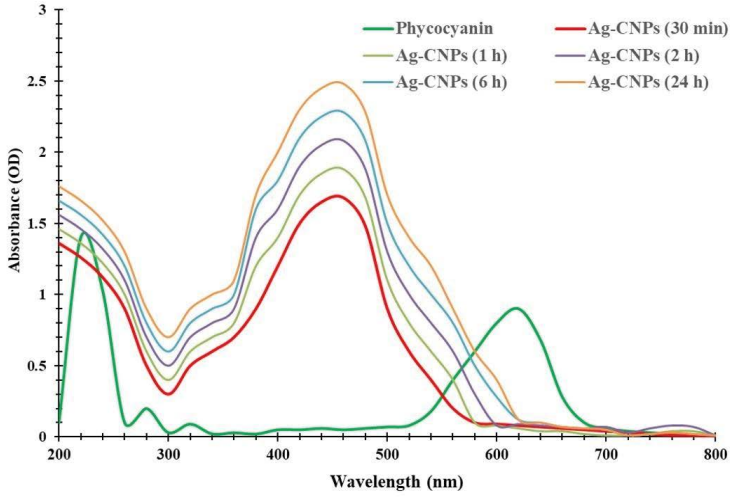

Figure 1 UV-VIS spectra recorded as a function of reaction time of an aqueous solution of 5 mM of $AgNO_3$ with the 10 ml of phycocyanin extract; the reaction time is indicated next to the respective curves

The optical properties of silver could be determined by a single Localized Surface Plasmon Resonances (LSPRs) effect. Phycocyanin-mediated Ag-CNPs showed a steady SPR peak in the UV spectra and retained their characteristic inherent yellowish-brown colour. It indicates that pigment-mediated synthesis is a sustainable green route to provide stable MNPs. Further, UV-visible spectrophotometric analysis of metal nanoparticles attained the maximum absorption at a wavelength peak of 440 nm indicating that incubation time is dependent on colour intensity which is due to Surface Plasmon Resonance (SPR) of AgNPs [29]. Reports on the production of pigment metallic nanoparticle synthesis are being found with *Monascus purpureus*, *Nostoc linckia,* and *Nostoc carneum* [30-33].

Characterization of Size, Shape, and Morphology of Ag-CNPs

Biosynthesized Ag-CNPs were characterized for their size, shape, and morphology by employing various analytical techniques, including X-ray Diffractometry (XRD), Fourier Transform Infrared Spectroscopy (FTIR), and Transmission Electron Microscopy.

X-ray Diffraction (XRD) Analysis

Crystalline size and structure of synthesized Ag-CNPs were determined by Bragg's reflection peaks, evident from the X-Ray diffraction pattern (Figure 2). Bragg's reflections peaks are observed at a 2θ value of 32.74º, 38.57º, 44.17º, 65.07º, and 78.02º which can correspond to (100), (111), (200), (220) and (311) lattice planes, respectively. This Face Cubic Centered (fcc) crystalline nature of nanoparticles is comparable with the reference pattern of Joint Committee on Powder Diffraction Standards (JCPDS) Card No. 04-0783 as shown in Figure 2.

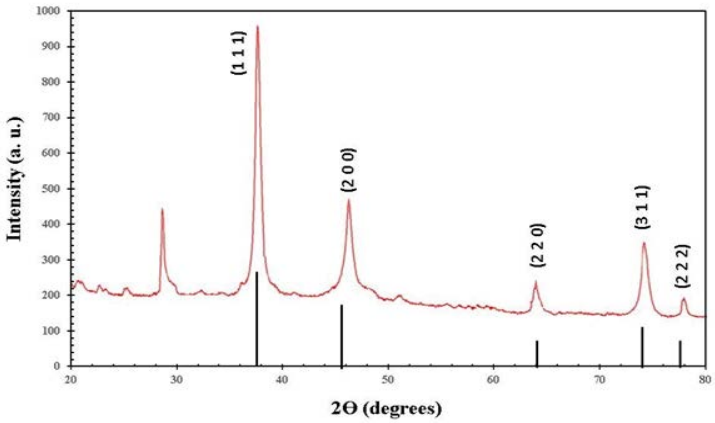

Figure 2 X-ray Diffraction for silver nanoparticles synthesized by using phycocyanin pigment

The mean crystallite size (L) of the material has been evaluated by Debye-Scherrer's formula ($L=K\lambda/\beta \cos\theta$) [34,35]. The XRD pattern thus clearly shows broadening of peaks, revealing the synthesis of crystalline Ag-CNPs by the reduction of Ag^{+} ions by phycocyanin within the nanometer range i.e., about 13.4 nm. An unassigned peak (marked with stars) was also observed suggesting that the crystallization of the bio-organic phase occurs on the surface of the silver nanoparticles. Similar results in silver nanoparticles synthesized using edible mushroom extract and also this similar result was reported by using geranium leaves [28,36]. Likewise, Xie also has found biosynthesis of AgNPs *via* extracts of *Chlorella vulgaris* hydroxyl and carboxyl groups are involved. XRD analysis of Ag-CNPs confirmed the presence of silver nanoparticles in crystalline shape and is confirmed by a peak at 111 (Figure 2) [37].

TEM, EDX, and Zeta Sizer Analysis

Transmission Electron Microscopy (TEM) was used to determine the particle size and morphology of the biosynthesized Ag-CNPs. TEM produces high-resolution, 2-Dimensional (2D) images by emission of energetic electrons on the samples. The TEM images confirmed the synthesis of spherical Ag-CNPs, a small width-to-length ratio with a 4 nm to 20.9 nm diameter range. The average size of spherical particles was 12.6 nm which also aggregates and forms clusters. This is also close to 13.4 nm, the crystalline size of Ag-CNPs, as estimated by Debye-Scherrer's formula. Furthermore, the inset of Figure 3 and Figure 4 shows Selected Area Electron Diffraction (SAED) patterns of crystalline and face-centred cubic structures, which is again in good agreement with the results obtained from XRD analysis. The formation of pits in the cell wall of *E. coli* was observed *via* TEM, finally affecting its cell integrity and causing apoptosis of the cell [38,39].

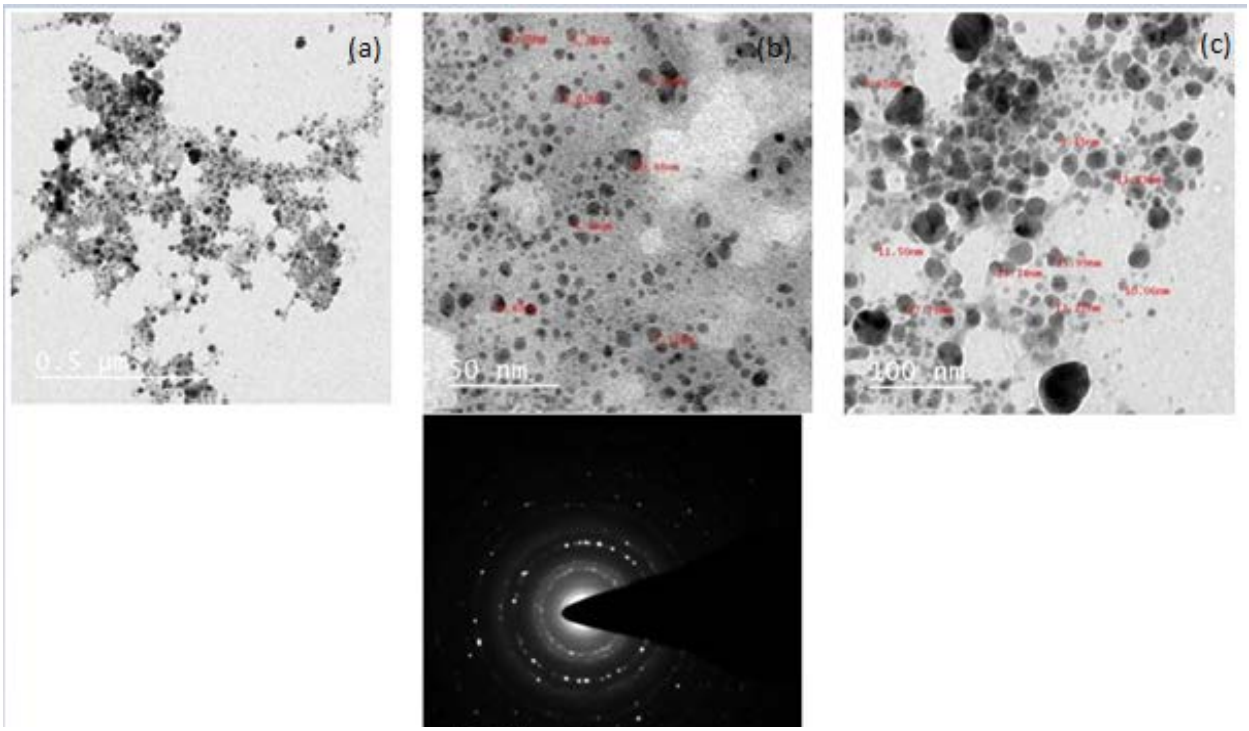

Figure 3 TEM micrograph showing the formation of Ag nanoparticles; TEM images and size distribution histogram of biosynthesized Ag NPs in which the scale bar represents at (a) 0.5 µm (b) 50 nm (c) 100 nm and (d) SAED pattern

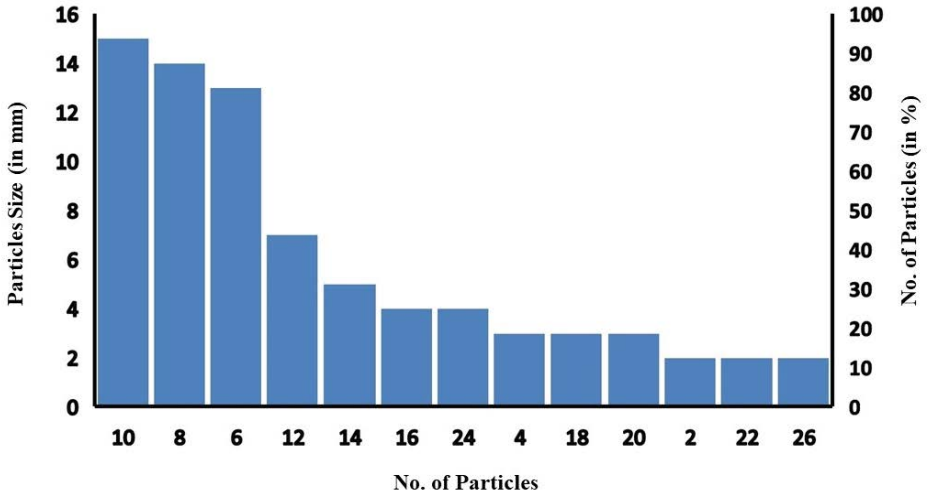

Figure 4 Particle size histogram analysis of AgNPs

The elemental composition of Ag-CNPs was examined by Energy Dispersive X-Ray Analysis (EDX). A spectrum of the energy versus relative counts of the detected x-rays is recorded and shown in Figure 5. EDX spectra proved the green synthesis of Ag-CNPs by phycocyanin, extracted from cyanobacterial cells and treated with $AgNO_3$ solution (Figure 5). In the middle part of the spectrum, the strongest characteristic maxima peaks of the Ag region can be observed in between 3 keV and 4 keV, due to surface plasmon resonance. This is by many researchers [40]. Additionally, carbon (C) and copper (Cu) elements peaks were also observed which ought to have come from carbon-coated copper grids for sample preparation. Weaker signals from Cl, O, P, Na, and Ca atoms confirm that synthesized Ag-CNPs were exclusively composed of silver. Zeta sizer analyses were also performed to determine surface zeta potential distribution and Polydispersity Index (PDI) of biosynthesized Ag-CNPs. Results showed Ag-CNPs biosynthesized from marine cyanobacteria have a negative zeta potential of -14.2 ± 3.17 mV with a conductivity of 0.310 mS/cm. It indicates moderate stability of NPs as particles with zeta potentials more positive than +30 mV or more negative than -30 mV are normally considered stable [41]. Moderate stable NPs with lower zeta potential are more benign from an environmental viewpoint because the existence of nanoparticles is shorter which indirectly minimizes the toxic effects of Ag-CNPs after utilization. Some researchers have also found that a negative zeta potential value of -13.1 mV indicated the stability and good dispersion of AgNPs [42]. The stability of Ag-CNPs was observed for up to 1 month at room temperature. No considerable changes in zeta potential were observed within the period studied. Sukhwal, et al. also found similar results with silver nanoparticles (AgNPs) synthesized using aqueous leaf extracts of *Tagetes patula* L. They showed that the zeta potential of AgNPs carries a charge of -14.2 mV up to 1 year and was stable at room temperature [43].

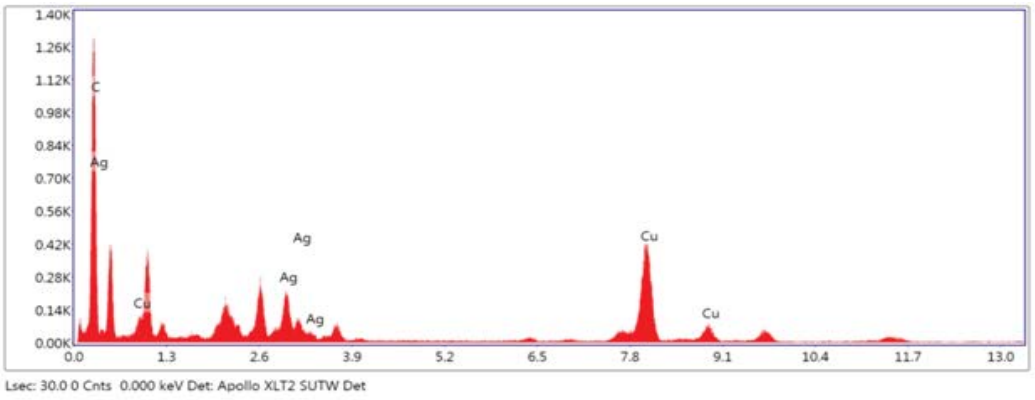

Figure 5 EDX spectrum recorded showing peak confirming the presence of silver nanoparticles synthesized from phycocyanin pigment

Polydispersity index for Ag-CNP was calculated as 0.81, indicating the heterogeneity of synthesized nanoparticle populations which can significantly influence the biodistribution and targeting efficiency of Ag-CNPs.

Fourier Transformed Infra-Red (FTIR) Spectroscopy Analysis

The bioorganic compounds bound on the surface of Ag-CNPs were determined by the FTIR spectrum (Figure 6). It helps to distinguish possible molecules responsible for the bio-reduction of Ag^{+} ions and capping of the bio-reduced Ag-CNPs by the phycocyanin extract. The FTIR spectrum of Ag-CNPs resulted in a peak extension from 3474/cm to 599/cm. It was observed that Ag-CNPs depicted functional groups at different wave numbers such as (3474, 3303, 1678, 1400, 1193, 1103, 984, 862, 768, and 599)/cm. The band at 3474/cm could be assigned to the N-H bond stretch found in aromatic amines, primary amines, and amides [44]. Subsequently, band at 3303/cm attributes to -NH bond found in protein and polysaccharide, O-H in oximes, and ≡CH-H stretch in acetylene [30]. The peak at 1678/cm is assigned to the presence of the C-N stretching vibration of aromatic amines [45]. In addition, the presence of bands at 1103/cm was assigned to C=S stretching in thiocarbonyl compounds. It showed a peak in the range of 984/cm relating to the C-N stretching vibration of primary amines, referring to the possible involvement of primary amines during nanoparticle synthesis [46]. The peak at 599 corresponds to -C-C-CN nitrites and C-C=O ketones. These functional groups may be responsible for capping and efficient stabilization of synthesized nanoparticles. Thus, the FTIR graph supports the presence of a specific type of protein on the surface of extracted phycocyanin, acts as capping agents, and is strongly involved in the reduction of silver ions during production which also prevents the reduced silver particles agglomeration.

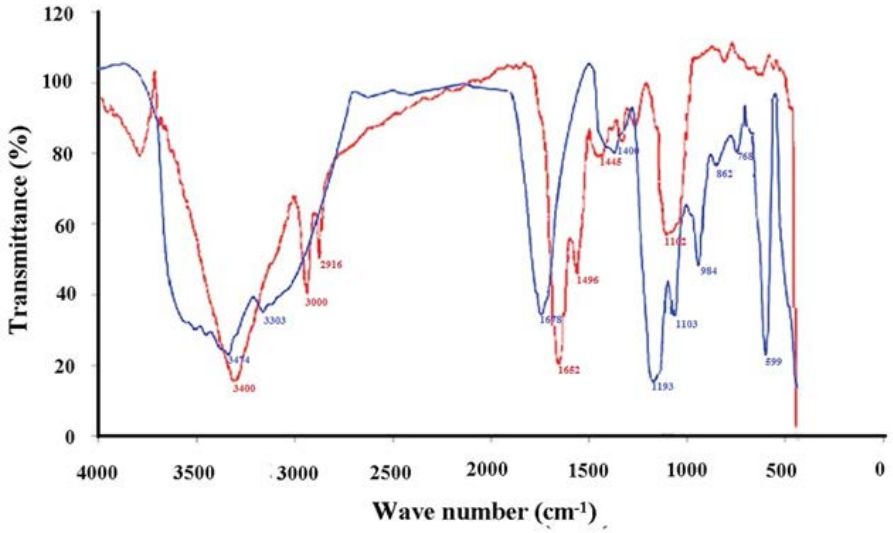

Figure 6 FTIR spectrum recorded by making KBr disc with synthesized silver nanoparticles by using phycocyanin pigment

Earlier reports are also in line with this study confirming the presence of carboxylic, amine, phosphate, and hydroxyl functional groups in the algal extract of *Sargassum polycystin* and are involved in the reduction of silver ions. Reports suggested that the stability of the AgNPs may be due to the presence of a protein that acts as a capping agent encapping and encapsulating the nanoparticles and forms a layer that prevents the nanoparticles from agglomeration [47]. Shaligram has shown that free amine groups of proteins can bind to AgNPs which is compatible with our studies [48]. FTIR measurements are widely employed for the precise identification of the possible functional groups for the stabilization of AgNPs [49]. FTIR spectrum is based on the surface chemistry of biosynthesized metal nanoparticles and implies an easy fact that material has unique characteristic absorptions in the IR spectrum. With the absorption of infrared rays, some vibrations of molecules can be recorded depending on their wavelength. These studies confirmed the identity of amino acids, carbonyl groups, and some synthesized proteins which act as stabilizing agents for the capping of AgNPs to prevent agglomeration of bio-green molecules in the reaction media [50].

Phycocyanin Synthesized Ag-CNPs Inhibit Bacterial Pathogens

Phycocyanin synthesized Ag-CNPs unveiled a wide range of inhibition spectrum activity against clinical pathogenic bacterial strains such as *Campylobacter* spp., *Shigella* sp., *Salmonella typhi*, *Bacillus subtilis,* and *Klebsiella* sp. The zone of bacterial inhibition is depicted in Figure 7 which demonstrates the potential of Ag-CNPs as clinical bactericidal applications. At 100 µg/mL Ag-CNPs concentration, nanoparticles showed the highest inhibition against *Klebsiella* (13.5 mm) and *B. subtilis* (13.3 mm) strains whereas the lowest zone of inhibition was observed against *Shigella* (8.0 mm). In addition, biosynthesized Ag-CNPs showed moderate inhibition against *Campylobacter*. However, the exact mechanism by which the Ag-CNPs exert their antibacterial effect remains to be elucidated. Based on these studies, Ag-CNPs may lead to important applications in different fields such as medicinal and antimicrobial agents. It is well recognized that silver and silver compounds are highly lethal to microbes [51]. To evaluate the broad-spectrum antimicrobial efficiency of the synthesized Ag-CNPs, an antibiotic susceptibility test was done on five bacteria. The synthesized Ag-CNPs are more efficient than the extract for inhibition of the growth of all pathogens (Gram-positive and Gram-negative). The effectiveness of the silver nanoparticle for bactericidal properties was not identical; it depends on the different pathogens [52]. *Klebsiella* and *Bacillus subtilis* are the most susceptible at 100 µg/mL Ag-CNPs and produce larger inhibition zones while *Shigella* is least with 25 µg/mL concentration of Ag-CNPs. Numerous research studies have been done to identify the antibacterial efficiency of biosynthesized AgNPs. Mechanisms of the bactericidal effects of AgNPs are still not known. *Spirulina platensis* mediated stable silver nanoparticles have been shown to have an inhibition zone of 1 nm-4 mm against *Staphylococcus* sp. and *Klebsiella* sp. [48]. Our results were in good agreement with that the increasing concentration of Ag-CNPs effectively reduced the bacterial density [53-55]. Research studies have indicated that silver metal nanoparticles smaller size inhibits bacterial growth which is by our results [52,56]. Reports by Singh suggest that the smaller size and crystalline structure of AgNPs have profound antimicrobial potential [57]. Entry into the bacteria is achieved *via* the negatively charged cell membrane bound by electrostatic forces of attraction. MNP after penetration leads to the disruption of its power functions like respiration and membrane depolarization thereby causing the production of reactive oxygen species and hence taking over the cellular machinery [58]. The size of the AgNPs plays an essential role in the determination of the bactericidal activity due to their penetration ability into the eukaryotic cells via active or passive uptake means. AgNPs are so small in size that they make their way into the bacterial cell and cause additional damage, affecting the intracellular processes at DNA, RNA levels via interacting with sulfur and phosphorus in DNA. The bactericidal property of AgNPs is largely dependent on the interaction surface. The smaller size AgNPs have a large surface area and provide more bactericidal activity than large size nanoparticles (Table 1) [59].

Figure 7 Antibacterial activities of silver nanoparticles by using phycocyanin pigment against bacterial species.

Table 1 Antibacterial activity of Ag-CNPs against pathogenic bacteria

S. No.	Name of the strains	Size of Inhibition			
		25 µg/mL Ag-CNPs (mm)	50 µg/mL Ag-CNPs (mm)	100 µg/mL Ag-CNPs (mm)	Control Ag-CNPs (mm)
1	*Campylobacter* sp.	9.0 ± 0.01	10.1 ± 0.01	12.3 ± 0.01	10 ± 1.3
2	*Shigella* sp.	8.1 ± 0.01	8.2 ± 0.01	10.3 ± 0.01	9 ± 1.2
3	*Salmonella typhi*	8.2 ± 0.01	9.5 ± 0.021	11.2 ± 0.01	8.2 ± 2.1
4	*Bacillus subtilis*	9.2 ± 0.01	10.2 ± 0.01	13.3 ± 0.01	8 ± 0.9
5	*Klebsiella pneumoniae*	8.5 ± 0.01	9.2 ± 0.01	13.5 ± 0.01	8.6 ± 1.7
± Values indicate the Standard Deviation (mean, n=3), mm: millimeter; C: Control					

Ag-CNPs Exert Anti-Proliferative Effect on MDA-MB-231 Cancer Cells

The cytotoxic effect of nanoparticles on the MDA-MB-231 cell line is illustrated in Figure 8. The cell viability and inhibition percentage of cell lines (replicates) were given in Table 2. Results revealed that synthesized Ag-CNPs were more cytotoxic when incubated for 72 hrs. For instance, at 1 µg/mL concentration, AgNPs showed a 16.85% growth inhibition in MDA-MB-231 cells; moreover, upon increasing the concentration of nanoparticles to 50 µg/mL, the growth was arrested (67%) with a potent cytotoxicity (IC_{50}) value of 46.47 µg/mL after 24 h. Likewise IC_{50} values for 48 hrs and 72 hrs were 5.84 µg/mL and 0.69 µg/mL. The proliferation rate was declined gradually with higher concentrations of (1-50 µg/mL) AgNPs and the viability of MDA-MB-231 cells gradually reduced from 80.15 ± 0.34% to 29.12 ± 0.11% , 41.42 ± 0.21% to 18.12 ± 0.28% and 25.12 ± 0.21% to 5.5 ± 0.12%, respectively, after 24, 48 and 72 hrs of incubation.

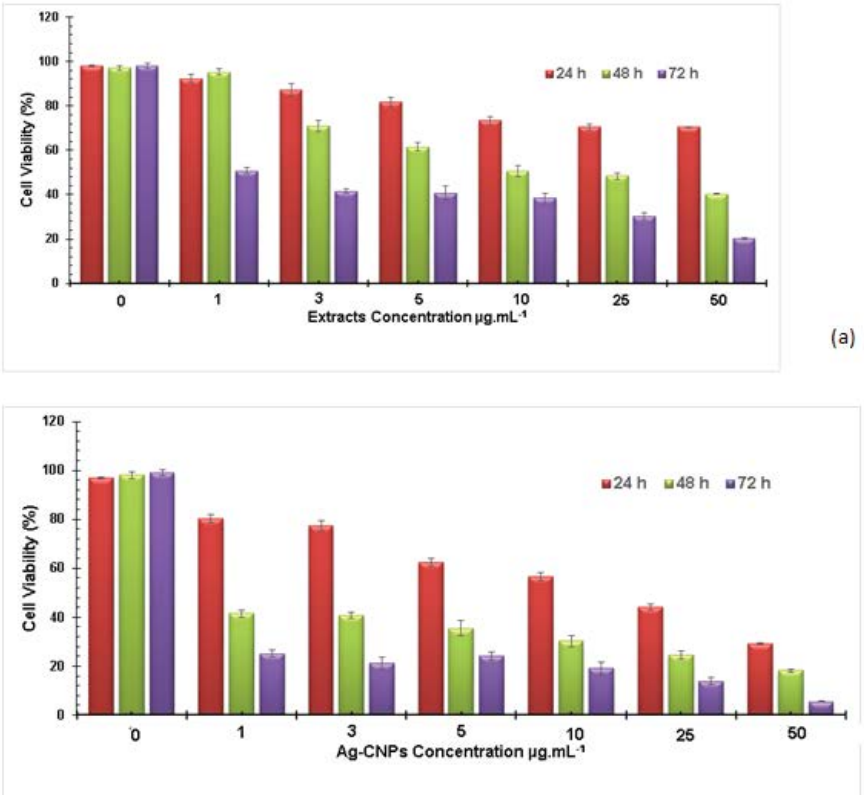

Figure 8 The mean percentage of cell viability of three replicates and standard deviation of MTT assay test values of MDA-MB-231 cell line after treatment for 24 hrs, 48 hrs, and 72 hrs with different concentrations of (a) phycocyanin extract and (b) biosynthesized AgNPs

Table 2 IC_{50} values of phycocyanin extract and PC @ Ag-CNPs against MDA-MBA-231 cell line

Time (hrs)	Extract (µg/ml)	Ag-CNPs (µg/ml)	DOX (µg/ml)
24	102.88	46.47	3.18
48	38.9	5.84	0.39
72	1.13	0.69	0.45

Data of ANOVA analysis revealed that all the values were significantly different, respectively. Research studies of inhibitory concentration (IC_{50}) for AgNPs against the breast cancer MCF-7 cell lines were found to be 27.79 ± 2.3 µg/mL [60]. The IC_{50} value of C-phycocyanin extract was 229.0 µg/mL with treatment for 24 h, while the IC_{50} value was 189.4 µg/mL after 48 h treatment [61]. Franco-Molina research reports that colloidal silver induced a dose-dependent cytotoxic effect on MDA-MB-231 breast cancer cells [29]. Silver nanoparticles synthesized using *Acalyphaindica Linn* aqueous extract exhibit 40% cytotoxicity of human breast cancer cells (MDA-MB-231) [46]. In the same context, Ag-CNPs formed by *Taxus baccata* aqueous extract showed effective anticancer potential against MCF-7 cells (IC_{50}=0.25 µg/mL) using MTT assay [32]. Viability tests are used to evaluate cytotoxicity that poses responses at the cellular level to toxic chemicals, which illustrate the importance of cell death, existence, and metabolic activity. There was a significant cytotoxic effect in a dose and time-dependent manner with a reduced survival rate. The cytotoxic effect induced by Ag-CNPs at minute concentrations determines its therapeutic potential in bringing about cell death. It was also anticipated that Ag-CNPs also increase ROS (Reactive Oxygen Species) causing oxidative stress harming vital enzymes and DNA resulting in DNA strand breaks and necrosis at higher concentrations [33]. In this present study, the anticancer potency of silver nanoparticles has shown dose-time-dependent cytotoxicity on MDA-MB-231 cells. The concentration of nanoparticles plays an essential role in drug effectiveness. In today's era, nano-medicine is a potential field that can lead to betterment in cancer therapy *via* early identification and proper distortion. Algal-derived nanoparticles play an important role in cancer cell lines [62-64]. Likewise, Ag-CNPs from *Allium autumnale* and *Acalyphaindica* leaf extracts have better cytotoxicity with MDA-MB 231 cell lines [31,65]. Studies on the mushroom synthesized silver nanoparticles have shown considerable cytotoxicity against MDA-MB-231 cell lines at somewhat low concentrations (6 µg/mL) [66]. Based on these studies, it is here speculated that the cytotoxicity of nanoparticles relies much on the nature of cell types and size of particles. Many researchers have also drawn similar conclusions. From the above study, it is evident that Ag-CNPs can be deployed as a potent anticancer agent in the future. Yet, before being given clinical applications, studies on animal models are mandatory to reveal the in vivo toxicity of Ag-CNPs.

Reactive Oxygen Species

The oxidative stress created in prokaryotic cells is known to play an important role in nanoparticles mediated cytotoxicity. The production of ROS intermediates during metal NPs interaction with bacterial cells causes oxidative stress, distortion of proteins and nucleic acids. The Ag-CNPs could then alter the functions of essential biomolecules like lipids, DNA, proteins, respiratory enzymes thereby causing oxidative stress hence liberating ROS and damage of nucleic acids and proteins, ultimately leading to the death of the bacterial cell [67,68]. The intracellular ROS generation in MDA-MB-231 cells was evaluated by DCFH-DA fluorescence staining. DCFH-DA dye is non-fluorescent but when internalized by cells in presence of ROS, the dye gets oxidized which emits green fluorescence due to DCFH [69]. Likewise, pronounced fluorescence means more ROS presence in the cells. This assay keeps a check for the intracellular generation of free radicals like hydroxyl, hydrogen peroxide, and peroxyl radicals so indirectly a measure for stress management. Figure 9 shows that concentrations of 19.45 µg/mL and 38.9 µg/mL could trigger the production of ROS. It can be seen that fluorescence intensity was increased with increasing concentration of Ag-CNPs and the incubation time which indicated concentration-dependent ROS activation leading to apoptosis of cells. The results of the quantitative estimation of ROS showed that 19.45 µg/mL of Ag-CNPs induced a 160.25% increment in ROS production when compared to untreated (control) cells. Moreover, ROS production was increased by 195.39% ($p<0.001$) at 38.9 µg/mL of Ag-CNPs compared to untreated (control) cells.

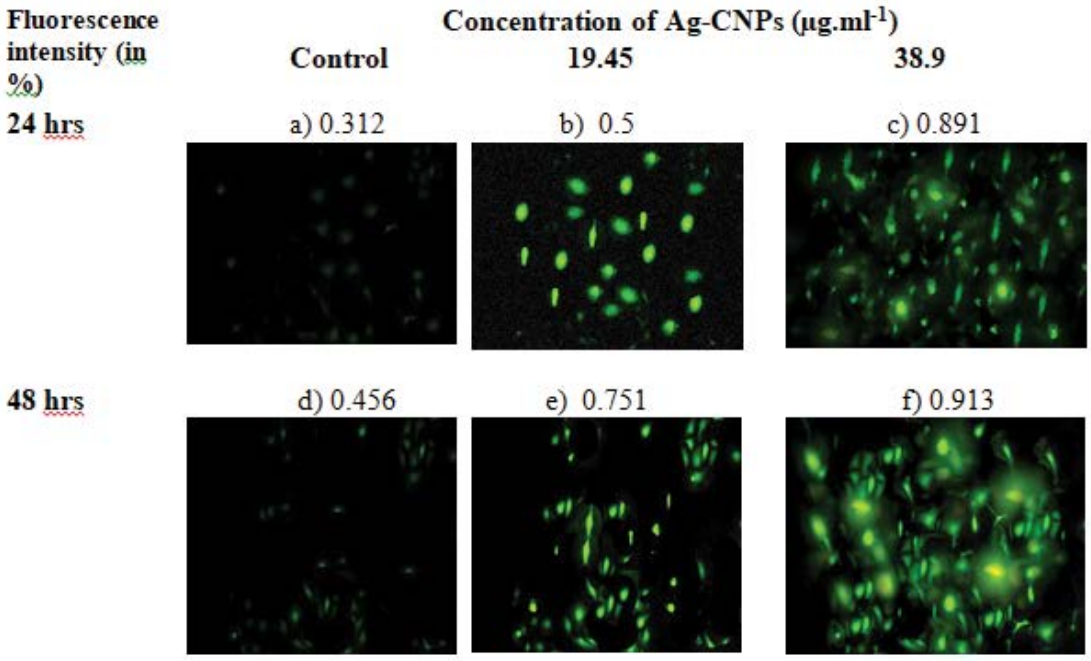

Figure 9 ROS generation in MDA-MB-231 cell line using silver nanoparticles under various experimental conditions as seen under a fluorescent microscope using DCFDA; a): Control cells for 24 hours; b): Cells treated for 24 hours with 19.45 µg/ml of Ag-CNPs; c): Cells treated for 24 hours with 38.9 µg/ml of Ag-CNPs; d): Control cells for 48 hours; e): Cells treated for 48 hours with 19.45 µg/ml of Ag-CNPs; f): Cells treated for 48 hours with 38.9 µg/ml of Ag-CNPs

CONCLUSION

In the present study, blue pigment phycocyanin, extracted from a marine cyanobacterial source was shown to be capable to biosynthesize Ag-CNPs. Biosynthesized nanoparticles appear to be an FCC crystalline pattern and spherical with a particle size of (4-20) nm. Ag-CNPs also have antibacterial activity against clinical bacterial pathogens. The highest zone of inhibition was achieved against *Klebsiella* (13.5 mm) *and B. subtilis* (13.3 mm) strains at 100 µg Ag-CNPs/mL concentrations. The cytotoxicity analysis of Ag-CNPs was also tested on MDA-MB-231 cancer cell lines. Results revealed that the proliferation rate of cancer cells declined gradually with higher (150 µg/mL-50 µg/mL) Ag-CNPs concentrations. Furthermore, the viability of MDA-MB-231 cells was also significantly reduced from 80.15% to 29.12%, 41.42% to 18.12%, and 25.12% to 5.5 %, respectively, after 24 hrs, 48 hrs, and 72 hrs. of incubation. Results were verified by quantitative estimation of reactive oxygen species which shows a 195.39% increase in ROS production with 38.9 µg/mL of Ag-CNPs, compared to control. It would be desirable to develop a green synthesis approach in which the small size and spherical shape of Ag-CNPs could be obtained by the use of cyanobacteria. Further research is needed to identify the mechanism of nanoparticle formation and compounds responsible for antibacterial and cytotoxic effects.

DECLARATIONS

Conflicts of Interest

The authors declared no potential conflicts of interest concerning the research, authorship, and/or publication of this article.

Acknowledgment

The authors are thankful to the University Grants Commission, New Delhi, India for providing D. Phil fellowship to Ms. Rupali Kaur and Dr. D. S Kothari Postdoctoral Fellowship (Grant Number: EN/19-20/0020) to Dr. Shailendra Kumar Singh for the financial assistance during the study period.

REFERENCES

[1] Aritonang, Henry F., Harry Koleangan, and Audy D. Wuntu. "Synthesis of silver nanoparticles using aqueous extract of medicinal plants' *(Impatiens balsamina* and *Lantana camara*) fresh leaves and analysis of antimicrobial activity." *International Journal of Microbiology,* Vol. 2019, 2019.

[2] Schneidewind, Henrik, et al. "The morphology of silver nanoparticles prepared by enzyme-induced reduction." *Beilstein Journal of Nanotechnology,* Vol. 3, No. 1, 2012, pp. 404-14.

[3] Huang, Zhongbing, et al. "Toxicological effect of ZnO nanoparticles based on bacteria." *Langmuir,* Vol. 24, No. 8, 2008, pp. 4140-44.

[4] Prasad, Tollamadugu NVKV, Venkata Subba Rao Kambala, and Ravi Naidu. "Phyconanotechnology: Synthesis of silver nanoparticles using brown marine algae *Cystophora moniliformis* and their characterisation." *Journal of Applied Phycology,* Vol. 25, No. 1, 2013, pp. 177-82.

[5] Rai, Mahendra, et al. "*Fusarium* as a novel fungus for the synthesis of nanoparticles: Mechanism and applications." *Journal of Fungi,* Vol. 7, No. 2, 2021, p. 139.

[6] Lengke, Maggy F., Michael E. Fleet, and Gordon Southam. "Morphology of gold nanoparticles synthesized by filamentous cyanobacteria from gold (I)-thiosulfate and gold (III)-chloride complexes." *Langmuir,* Vol. 22, No. 6, 2006, pp. 2780-87.

[7] Lengke, Maggy F., et al. "Mechanisms of gold bioaccumulation by filamentous cyanobacteria from gold (III)-chloride complex." *Environmental Science & Technology,* Vol. 40, No. 20, 2006, pp. 6304-09.

[8] Brayner, Roberta, et al. "Cyanobacteria as bioreactors for the synthesis of Au, Ag, Pd, and Pt nanoparticles *via* an enzyme-mediated route." *Journal of Nanoscience and Nanotechnology,* Vol. 7, No. 8, 2007, pp. 2696-708.

[9] Govindaraju, K., et al. "Extracellular synthesis of silver nanoparticles by a marine alga, *Sargassum wightii* Grevilli and their antibacterial effects." *Journal of Nanoscience and Nanotechnology,* Vol. 9, No. 9, 2009, pp. 5497-501.

[10] Chakraborty, Nabanita, et al. "Biorecovery of gold using cyanobacteria and an eukaryotic alga with special reference to nanogold formation-A novel phenomenon." *Journal of Applied Phycology,* Vol. 21, No. 1, 2009, pp. 145-52.

[11] Parial, Dipannita, et al. "Gold nanorod production by cyanobacteria-A green chemistry approach." *Journal of Applied Phycology,* Vol. 24, No. 1, 2012, pp. 55-60.

[12] Parial, D., and R. Pal. "Green synthesis of gold nanoparticles using cyanobacteria and their characterization." *Indian Journal of Applied Research,* Vol. 4, 2014, pp. 69-72.

[13] Lenartowicz, Monika, et al. "Formation of variously shaped gold nanoparticles by *Anabaena laxa*." *Journal of Cluster Science,* Vol. 28, No. 5, 2017, pp. 3035-55.

[14] Ameen, Fuad, et al. "Fabrication of silver nanoparticles employing the cyanobacterium *Spirulina platensis* and its bactericidal effect against opportunistic nosocomial pathogens of the respiratory tract." *Journal of Molecular Structure,* Vol. 1217, 2020, p. 128392.

[15] Ali, D. Mubarak, et al. "Biosynthesis and characterization of silver nanoparticles using marine cyanobacterium, *Oscillatoria willei* NTDM01." *Digest Journal of Nanomaterials and Biostructures,* Vol. 6, No. 2, 2011, pp. 385-90.

[16] Soni, Badrish, et al. "Extraction, purification and characterization of phycocyanin from *Oscillatoria quadripunctulata*-Isolated from the rocky shores of Bet-Dwarka, Gujarat, India." *Process Biochemistry,* Vol. 41, No. 9, 2006, pp. 2017-23.

[17] Liao, Xiaoxia, et al. "Purification of C-phycocyanin from *Spirulina platensis* by single-step ion-exchange chromatography." *Chromatographia,* Vol. 73, No. 3, 2011, pp. 291-96.

[18] Lowry, Oliver H., et al. "Protein measurement with the Folin phenol reagent." *Journal of Biological Chemistry,* Vol. 193, 1951, pp. 265-75.

[19] Bennett, Allen, and Lawrence Bogorad. "Complementary chromatic adaptation in a filamentous blue-green alga." *Journal of Cell Biology,* Vol. 58, No. 2, 1973, pp. 419-35.

[20] Silveira, Silvana Terra, et al. "Optimization of phycocyanin extraction from *Spirulina platensis* using factorial design." *Bioresource Technology,* Vol. 98, No. 8, 2007, pp. 1629-34.

[21] Stepanek, P. "Dynamic light scattering: The method and some applications." *W. Brown, Clarendon Press Oxford,* 1993, p. 177.

[22] Corbett, Jason CW, et al. "Measuring surface zeta potential using phase analysis light scattering in a simple dip cell arrangement." *Colloids and Surfaces A: Physicochemical and Engineering Aspects,* Vol. 396, 2012, pp. 169-76.

[23] Nathan, Paul, et al. "A laboratory method for selection of topical antimicrobial agents to treat infected burn wounds." *Burns,* Vol. 4, No. 3, 1978, pp. 177-87.

[24] Van Meerloo, Johan, Gertjan JL Kaspers, and Jacqueline Cloos. "Cell sensitivity assays: The MTT assay." *Cancer Cell Culture*, Humana Press, 2011, pp. 237-45.

[25] Tolosa, Laia, Maria Teresa Donato, and Maria Jose Gomez-Lechon. "General cytotoxicity assessment by means of the MTT assay." *Protocols in in vitro hepatocyte research*, 2015, pp. 333-48.

[26] Siddiqui, Sahabjada, et al. "*Cissus quadrangularis* Linn exerts dose-dependent biphasic effects: Osteogenic and anti-proliferative, through modulating ROS, cell cycle and Runx2 gene expression in primary rat osteoblasts." *Cell Proliferation,* Vol. 48, No. 4, 2015, pp. 443-54.

[27] Paramelle, David, et al. "A rapid method to estimate the concentration of citrate capped silver nanoparticles from UV-visible light spectra." *Analyst,* Vol. 139, No. 19, 2014, pp. 4855-61.

[28] Nabikhan, Asmathunisha, et al. "Synthesis of antimicrobial silver nanoparticles by callus and leaf extracts from saltmarsh plant, *Sesuvium portulacastrum* L." *Colloids and Surfaces B: Biointerfaces,* Vol. 79, No. 2, 2010, pp. 488-93.

[29] Franco-Molina, Moises A., et al. "Antitumor activity of colloidal silver on MCF-7 human breast cancer cells." *Journal of Experimental & Clinical Cancer Research,* Vol. 29, No. 1, 2010, pp. 1-7.

[30] Awad, T. S., et al. "Applications of ultrasound in analysis, processing and quality control of food: A review." *Food Research International,* Vol. 48, No. 2, 2012, pp. 410-27.

[31] Krishnaraj, C., et al. "*Acalypha indica* Linn: Biogenic synthesis of silver and gold nanoparticles and their cytotoxic effects against MDA-MB-231, human breast cancer cells." *Biotechnology Reports,* Vol. 4, 2014, pp. 42-49.

[32] Kajani, Abolghasem Abbasi, et al. "Green synthesis of anisotropic silver nanoparticles with potent anticancer activity using *Taxus baccata* extract." *Rsc Advances,* Vol. 4, No. 106, 2014, pp. 61394-403.

[33] Fu, Peter P., et al. "Mechanisms of nanotoxicity: Generation of reactive oxygen species." *Journal of Food and Drug Analysis,* Vol. 22, No. 1, 2014, pp. 64-75.

[34] Vidhu, V. K., S. Aswathy Aromal, and Daizy Philip. "Green synthesis of silver nanoparticles using *Macrotyloma uniflorum*." *Spectrochimica Acta Part A: Molecular and Biomolecular Spectroscopy,* Vol. 83, No. 1, 2011, pp. 392-97.

[35] Philip, Daizy. "Biosynthesis of Au, Ag and Au-Ag nanoparticles using edible mushroom extract." *Spectrochimica Acta Part A: Molecular and Biomolecular Spectroscopy,* Vol. 73, No. 2, 2009, pp. 374-81.

[36] Shankar, S. Shiv, Absar Ahmad, and Murali Sastry. "Geranium leaf assisted biosynthesis of silver nanoparticles." *Biotechnology Progress,* Vol. 19, No. 6, 2003, pp. 1627-31.

[37] Xie, Jianping, et al. "Silver nanoplates: From biological to biomimetic synthesis." *ACS Nano,* Vol. 1, No. 5, 2007, pp. 429-39.

[38] Raffi, M., et al. "Antibacterial characterization of silver nanoparticles against *E. coli* ATCC-15224." *Journal of*

Materials Science and Technology, Vol. 24, No. 2, 2008, pp. 192-96.

[39] Sondi, Ivan, and Branka Salopek-Sondi. "Silver nanoparticles as antimicrobial agent: A case study on *E. coli* as a model for Gram-negative bacteria." *Journal of Colloid and Interface Science* Vol. 275, No. 1, 2004, pp. 177-82.

[40] Vanaja, Mahendran, et al. "Phytosynthesis of silver nanoparticles by *Cissus quadrangularis*: Influence of physicochemical factors." *Journal of Nanostructure in Chemistry,* Vol. 3, No. 1, 2013, pp. 1-8.

[41] Hunter, Robert J. "Zeta potential in colloid science: Principles and applications." Vol. 2, Academic press, 2013.

[42] Jebril, Siwar, Raoudha Khanfir Ben Jenana, and Chérif Dridi. "Green synthesis of silver nanoparticles using *Melia azedarach* leaf extract and their antifungal activities: *In vitro* and i*n vivo*." *Materials Chemistry and Physics,* Vol. 248, 2020, p. 122898.

[43] Sukhwal, Aradhana, et al. "Biosynthesised silver nanoparticles using aqueous leaf extract of *Tagetes patula* L. and evaluation of their antifungal activity against phytopathogenic fungi." *IET Nanobiotechnology,* Vol. 11, No. 5, 2017, pp. 531-37.

[44] Devaraj, Preetha, et al. "Synthesis and characterization of silver nanoparticles using cannonball leaves and their cytotoxic activity against MCF-7 cell line." *Journal of Nanotechnology,* Vol. 2013, 2013.

[45] Dauthal, Preeti, and Mausumi Mukhopadhyay. "Biosynthesis of palladium nanoparticles using *Delonix regia* leaf extract and its catalytic activity for nitro-aromatics hydrogenation." *Industrial & Engineering Chemistry Research,* Vol. 52, No. 51, 2013, pp. 18131-39.

[46] Emmanuel, R., et al. "Green synthesis of gold nanoparticles for trace level detection of a hazardous pollutant (nitrobenzene) causing Methemoglobinaemia." *Journal of Hazardous Materials,* Vol. 279, 2014, pp. 117-24.

[47] Chandran, S. Prathap, et al. "Synthesis of gold nanotriangles and silver nanoparticles using Aloevera plant extract." *Biotechnology Progress,* Vol. 22, No. 2, 2006, pp. 577-83.

[48] Shaligram, Nikhil S., et al. "Biosynthesis of silver nanoparticles using aqueous extract from the compactin producing fungal strain." *Process Biochemistry,* Vol. 44, No. 8, 2009, pp. 939-43.

[49] Noginov, M. A., et al. "The effect of gain and absorption on surface plasmons in metal nanoparticles." *Applied Physics B,* Vol. 86, No. 3, 2007, pp. 455-60.

[50] Bagherzade, Ghodsieh, Maryam Manzari Tavakoli, and Mohmmad Hasan Namaei. "Green synthesis of silver nanoparticles using aqueous extract of saffron (*Crocus sativus* L.) wastages and its antibacterial activity against six bacteria." *Asian Pacific Journal of Tropical Biomedicine,* Vol. 7, No. 3, 2017, pp. 227-33.

[51] Gong, Yinyan, et al. "Origin of defect-related green emission from ZnO nanoparticles: Effect of surface modification." *Nanoscale Research Letters,* Vol. 2, No. 6, 2007, pp. 297-302.

[52] Shrivastava, Siddhartha, et al. "Characterization of enhanced antibacterial effects of novel silver nanoparticles." *Nanotechnology,* Vol. 18, No. 22, 2007, p. 225103.

[53] Sudhakar, Chinnappan, et al. "*Acorus calamus* rhizome extract mediated biosynthesis of silver nanoparticles and their bactericidal activity against human pathogens." *Journal of Genetic Engineering and Biotechnology,* Vol. 13, No. 2, 2015, pp. 93-99.

[54] Selvam, Kandasamy, et al. "Eco-friendly biosynthesis and characterization of silver nanoparticles using *Tinospora cordifolia* (Thunb.) Miers and evaluate its antibacterial, antioxidant potential." *Journal of Radiation Research and Applied Sciences,* Vol. 10, No. 1, 2017, pp. 6-12.

[55] Govarthanan, Muthusamy, et al. "Low-cost and eco-friendly synthesis of silver nanoparticles using coconut (*Cocos nucifera*) oil cake extract and its antibacterial activity." *Artificial Cells, Nanomedicine, and Biotechnology,* Vol. 44, No. 8, 2016, pp. 1878-82.

[56] Martins, Dorival, et al. "Antitumoral activity of L-ascorbic acid-poly-D, L-(lactide-co-glycolide) nanoparticles containing violacein." *International Journal of Nanomedicine,* Vol. 5, 2010, pp. 77-85.

[57] Singh, Garvita, et al. "Green synthesis of silver nanoparticles using cell extracts of *Anabaena doliolum* and screening of its antibacterial and antitumor activity." *Journal of Microbiology and Biotechnology,* Vol. 24, No. 10, 2014, pp. 1354-67.

[58] Dibrov, Pavel, et al. "Chemiosmotic mechanism of antimicrobial activity of Ag+ in *Vibrio cholerae*." *Antimicrobial Agents and Chemotherapy,* Vol. 46, No. 8, 2002, pp. 2668-70.

[59] Ibrahim, Haytham MM. "Characterization of silver nanoparticles using banana peel extract and their antimicrobial activity against representative microorganisms." *Journal of Radiation Research and Applied Sciences,* Vol. 8, No. 3, 2015, pp. 265-75.

[60] El-Naggar, Noura El-Ahmady, Mervat H. Hussein, and Asmaa Atallah El-Sawah. "Phycobiliprotein-mediated synthesis of biogenic silver nanoparticles, characterization, *in vitro* and *in vivo* assessment of anticancer activities." *Scientific Reports,* Vol. 8, No. 1, 2018, pp. 1-20.

[61] Jiang, Liangqian, et al. "C-Phycocyanin exerts anti-cancer effects via the MAPK signaling pathway in MDA-MB-231 cells." *Cancer Cell International,* Vol. 18, No. 1, 2018, pp. 1-14.

[62] Devi, J. S., B. V. Bhimba, and K. Ratnam. "Anticancer activity of silver nanoparticles synthesized by the seaweed *Ulva lactuca in vitro*." *Scientific Reports,* Vol. 1, No. 4, 2012, p. 242.

[63] Roychoudhury, Piya, et al. "Cyanobacteria assisted biosynthesis of silver nanoparticles-A potential antileukemic agent." *Journal of Applied Phycology,* Vol. 28, No. 6, 2016, pp. 3387-94.

[64] Ebrahiminezhad, Alireza, et al. "Biomimetic synthesis of silver nanoparticles using microalgal secretory carbohydrates as a novel anticancer and antimicrobial." *Advances in Natural Sciences: Nanoscience and Nanotechnology,* Vol. 7, No. 1, 2016, p. 015018.

[65] Isbilen, Ovgu, Nahit Rizaner, and Ender Volkan. "Anti-proliferative and cytotoxic activities of *Allium autumnale* PH Davis (Amaryllidaceae) on human breast cancer cell lines MCF-7 and MDA-MB-231." *BMC Complementary and Alternative Medicine,* Vol. 18, No. 1, 2018, pp. 1-13.

[66] Gurunathan, Sangiliyandi, et al. "Green synthesis of silver nanoparticles using Ganoderma neo-*japonicum* Imazeki: A potential cytotoxic agent against breast cancer cells." *International Journal of Nanomedicine,* Vol. 8, 2013, pp. 4399-413.

[67] Morones, Jose Ruben, et al. "The bactericidal effect of silver nanoparticles." *Nanotechnology,* Vol. 16, No. 10, 2005, p. 2346.

[68] Lara, Humberto H., et al. "Bactericidal effect of silver nanoparticles against multidrug-resistant bacteria." *World Journal of Microbiology and Biotechnology,* Vol. 26, No. 4, 2010, pp. 615-21.

[69] Ramalingam, Baskaran, Thanusu Parandhaman, and Sujoy K. Das. "Antibacterial effects of biosynthesized silver nanoparticles on surface ultrastructure and nanomechanical properties of gram-negative bacteria *viz. Escherichia coli* and *Pseudomonas aeruginosa*." *ACS Applied Materials & Interfaces,* Vol. 8, No. 7, 2016, pp. 4963-76.